Sensing and Discrimination of Explosives at Variable Concentration with a Large-Pore MOF as part of a Luminescent Array

Monika Jurcic[†,∞], William J Peveler[‡,∞,], Christopher N Savory[†], Dejan-Krešimir Bučar[†], Anthony J Kenyon[♦], David O Scanlon[†,∇] and Ivan P Parkin[†].*

† Department of Chemistry, University College London, 20 Gordon Street, London, WC1H 0AJ, UK.

‡ Division of Biomedical Engineering, School of Engineering, College of Science and Engineering, University of Glasgow, Glasgow G12 8LT, UK

♦ Department of Electronic and Electrical Engineering, University College London, WC1E 7JE, UK.

∇ Diamond Light Source Ltd., Diamond House, Harwell Science and Innovation Campus, Didcot, Oxfordshire OX11 0DE, UK

Keywords: explosive, metal-organic framework, array, luminescence, discriminant analysis, PETN

Metal-organic frameworks (MOFs) have shown great promise for sensing of dangerous chemicals, including environmental toxins, nerve agents and explosives. However, challenges remain, such as the sensing of larger analytes and the discrimination between similar analytes at different concentrations. Herein we present the synthesis and development of a new, large-pore MOF for explosives sensing, and demonstrate its excellent sensitivity against a range of relevant explosive compounds including trinitrotoluene (TNT) and pentaerythritol tetranitrate (PETN). We have developed an improved, thorough methodology to eliminate common sources of error in our sensing protocol. We then combine this new MOF with two others as part of a three-MOF array for fluorescent sensing and discrimination of five explosives. This sensor works at part-per-million concentrations and importantly, can discriminate explosives with high accuracy without reference to their concentration.

Introduction

Fluorescence-based sensing of explosives has been repeatedly demonstrated as a useful tool for homeland security and environmental safety applications.[1] Indeed, several systems are now successfully commercialized as detection tools.[1-3] The advantages of using fluorescence for detecting explosives include sensitivity, due to the very electron withdrawing nature of the explosive molecules; the ability to detect a wide range of different explosives by tuning the fluorescent material in question; and the simplicity and robustness of the detection method, over techniques such as mass spectrometry or ion-mobility spectrometry. Fluorescent materials previously used to detect explosives include polymers,[4] small molecules,[5,6] nanoparticles[7,8] and nanoporous materials such as metal organic frameworks (MOFs).[9,10]

In particular, MOF-based sensors for explosives have seen success in recent years due to their tuneable porosity, variation in the mechanism of interaction with the explosive (through

organic linker or metal center-based quenching) and hugely customizable structures.[11] MOFs have successfully been used to detect nitro-aromatics such as picric acid and trinitrotoluene (TNT) in solution and vapor phase respectively as well as explosive related vapors such as taggant DMNB, through "turn-off" luminescent detection.[12] Turn-off detection is so named because the MOF luminescence is strongly quenched by the very electron withdrawing materials in nitro-explosives, but not by other common interferants containing other functional groups or fewer nitro groups.[11]

However, an unmet challenge is to design MOFs that can sense larger nitroaliphatic explosives such as pentaerythritol tetranitrate (PETN). Another issue that is frequently encountered using 'turn-off' luminescent detection in MOFs and many other sensor materials, is the question of explosive discrimination – detecting, and then putting a name to the explosive detected. This requires the sensor to give a different response to each explosive encountered, that goes beyond a simple intensity change. The problem arises from the fact that if a simple quench value is used, for example 50 ppm TNT quenches the MOF by 50% of its initial intensity, then another explosive at a different concentration may give the same outcome. Dinitrotoluene (DNT) at, say, 150 ppm might also quench the MOF by 50%. Thus, we can say an explosive is almost certainly present but have no certainty of what it might be.

A method developed to overcome this problem is the 'discriminatory array'; based loosely on the operating mechanism of the mammalian nose, using several sensor elements that respond differently to different analytes, thus providing a 'fingerprint' for each analyte.[13] In this way the two explosives (or more) may be differentiated even if present at different concentrations based on their differing molecular structure and interactions.[7,14] This concept has been successfully demonstrated using nanoparticle sensors for explosives amongst others,

however previous examples of MOFs used in arrays are limited.[15] Previous research by Li *et al.* sought to discriminate between the compounds introduced to a flexible metal-organic framework ($[Zn_2(ndc)_2(bpee)\bullet 2.25DMF\ 0.5H_2O]$) by monitoring both the changes in fluorescence intensity and emission frequency (spectral) shift of the MOF upon exposure to the analytes.[16] Although this work effectively demonstrated how utilizing both of these variables in signal transduction can increase the discrimination of analytes using a single MOF system; some analytes still yielded similar responses of the MOF despite being chemically different. Therefore, the discrimination of these analytes is still not possible if varying their concentrations.

Two other reports exist on the use of MOFs in sensor arrays for other applications. Research by Dincă *et al.* demonstrated the effective detection and identification of volatile organic compounds (VOCs) using an array of chemiresistive rather than fluorescent MOFs,[17] and Wilmer et al. reported the computational screening of different MOF arrays (based on gas adsorption predictions) with aim to gain insight into which MOFs are most effective for use in a MOF gas sensing array.[18]

To simultaneously address the need for larger pored, explosive responsive MOFs and improve explosive discrimination, in this study we sought to create and test a MOF that had large enough pores to enable the detection the under-researched nitroaliphaitcs. We undertook a rational design process, selecting an isoreticular structural modification of an existing MOF structures and exchanging the metal ion to ensure the MOF was fluorescent, whilst maintaining porosity. This was tested, in combination with computer modelling of the MOF energy levels and an improved solution phase sensing protocol to successfully detect PETN and Tetryl with good limits of detection (ppm). We then developed this MOF as part of a 3 MOF array, for the luminescent detection and discrimination of five explosives at a range of concentrations. We

demonstrate how this technique can operate, even without prior knowledge of the concentration of the explosive in question.

Results and Discussion

The MOF **MJ3** was designed to have large pore volume and still retain porosity and fluorescent properties for the sensing of larger explosive analytes.

In previous work, Eddaoudi *et al.* synthesized metal-organic framework $[Cu_4L(H_2O)_4•(solvent)]_n$, ($H_8L$ = 5,5',5",5"'-[1,2,4,5-benzenetetrayltetrakis(methyleneoxy)]tetra-1,3-benzenedicarboxylic acid) which exhibits the same *tbo* net as the prototypical MOF HKUST-1 ($[Cu_3(BTC)_2]$, H_2BTC = benzene-1,3,5-tricarboxylic acid). HKUST-1 is one of few industrially manufactured metal-organic frameworks,[19] and has shown promise for suitability in a number of commercial applications, namely catalysis.[20] The popularity of this MOF arises from its reported chemical stability coupled with its high permanent porosity (BET surface areas are typically in the range of 600 - 1600 m^2g^{-1}).[21] The structures of both $[Cu_4L(H_2O)_4•(solvent)]_n$ and HKUST-1 and the linkers by which they are synthesized have underlying (3,4)-coordination, the paddle-wheel SBUs in both of these MOFs have four points of extension and the linkers are three connectivity branch points.[22]

MOF $[Cu_4L(H_2O)_4•(solvent)]_n$ contains larger pore apertures than HKUST-1 (Langmuir apparent surface area was calculated to be 2896 m^2 g^{-1}), is synthesized with a flexible and fluorescent linker and similarly to HKUST-1 has the potential through dehydration to contain un-coordinated metal sites (UMS). New MOF $[Zn_4L(H_2O)_4•(solvent)]_n$, (**MJ3**), was based on the Cu framework of Eddaoudi *et al.*[23] with the variation between the two being the metal with which they are constructed. MOF **MJ3** is isoreticular to Eddaoudi's MOF and HKUST-1, but displays photoluminesence.

Synthesis, Characterization and Activation of MJ3.

The MOF **MJ3** was synthesized from a DMF solution of H_8L and $Zn(NO_3)_2 \cdot 6H_2O$ as described in the Methods section and shown in **Figure 1a**. From the resulting crystalline material, a clear, suitably-sized and block-shaped crystal was used for single crystal X-ray diffraction studies.

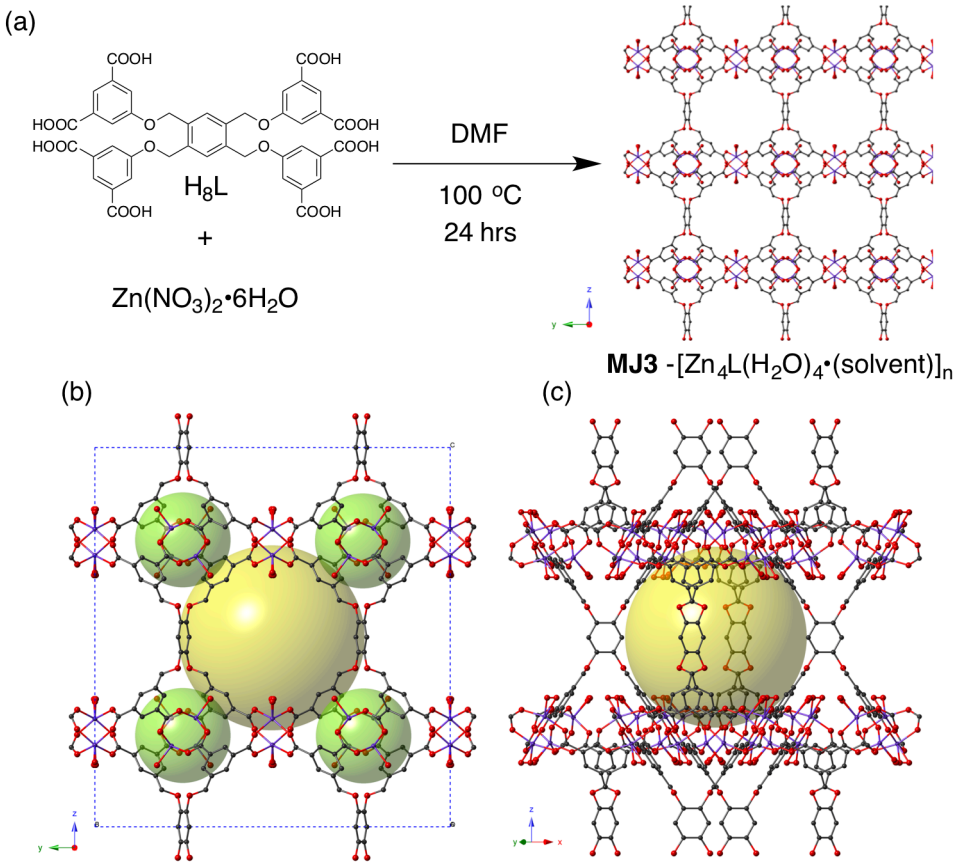

Figure 1. (a) Synthesis for **MJ3**, showing an extended 3D representation viewed along the crystallographic *a*-axis. (b) **MJ3** unit cell structure showing the two different pore environments (green and yellow spheres). The smallest portal opening for the largest (yellow) cavity is 15 Å in diameter, based on Van der Waal's radii and including hydrogen atoms. (c) Alternative view of the unit cell, showing the largest pore (yellow sphere). In all models, hydrogen atoms have been omitted for clarity.

Structural analyses revealed that MOF **MJ3** is isomorphous with the $[Cu_4L(H_2O)_4•(solvent)]_n$ MOF reported by the Eddaoudi group (**Table S2**).[23] In particular, **MJ3** crystallizes as $[Zn_4L(H_2O)_4•(solvent)]_n$ in the orthorhombic space group *Fmmm* with two zinc(II) ions, two coordinating water molecules and one quarter of the L^{8-} ligand in the asymmetric unit (**Figure S1**). The three-dimensional **MJ3** framework features dinuclear $Zn_2(carboxylate)_4$ paddle-wheel clusters that act as 4-connected node. The zinc(II) ions in each paddlewheel exhibit a square-pyramidal geometry wherein four oxygen atoms (belonging to four carboxylate moieties of separate L^{8-} ligands) coordinate a zinc(II) ion. The fifth apical position of the square pyramid is occupied by a water molecule. The paddle-wheel units are linked by L^{8-} ligands into a framework that exhibits a *tbo* topology, whereby the benzene moieties of the ligand serve as a 4-connected nodes and its 5-*R*-isophthalate moieties act as 3-connected nodes. The **MJ3** framework exhibits solvent-accessible areas that take up nearly 70% of the unit cell volume, which is marginally lower than the 72% solvent-accessible volume reported for the copper analogue of the Eddaoudi Group.[23] The content of the solvent content of the solvent-accessible space could not be determined crystallographically since all guest molecules exhibited high degrees of disorder. The crystal structure of **MJ3** was therefore refined using a solvent-mask procedure. Details pertaining to the structure solution and refinement are described in the **Supplement Information** document (**Table S1**).

A four stage washing procedure was implemented for the removal of coordinating DMF solvent from the pores of **MJ3** to yield the "activated" framework **MJ3'** ($[Zn_4L(H_2O)_4]_n$, that would respond to analytes now able to enter the MOF pores. The PXRD patterns of the crystalline material present after each stage of the washing procedure are shown in **Figure S2**. The diffraction patterns were obtained with each of the crystals *in-situ*, that is immersed in the solution they were being washed with, with the exception of the final pattern, which shows **MJ3'**

post solvent evacuation at room temperature under dynamic vacuum. The overall structure of this MOF remains intact during the implemented washing procedure demonstrated by the retention of the main MOF peaks in the PXRD pattern, and thus overall porosity is maintained.

The excitation spectrum of the MOF **MJ3'** suspension in MeCN indicated this framework to best excited at wavelength λ_{ex} = 315 nm (**Figure 2**), therefore, all sensing experiments were conducted at this wavelength. The fluorescence emission maxima of MOF **MJ3'** in MeCN was observed to be λ_{em} = 348 nm, whereas that of the linker H_8L (dissolved in DMF) was 335 nm (λ_{ex} = 315 nm). This observed red-shift in the excitation and emission spectrum of the free linker and the MOF is very typical of organic ligands being incorporated into MOFs, and is usually ascribed to the electronic coupling of the neighboring organic ligands in the framework through the metal ions,[24] as well as increased scattering from the particulate suspension. The electronic coupling is further evidenced by the presence of a second band arising at c. 340 nm in the absorption/extinction spectrum, coinciding with the MOF excitation maximum. The final Stokes shift was similar to or larger than many organic dyes, and reduced the effects of self-absorption. Quantum yield measurements were difficult to obtain accurately due to the UV absorption and scattering by the MOF solution (discussion in Supporting Information).

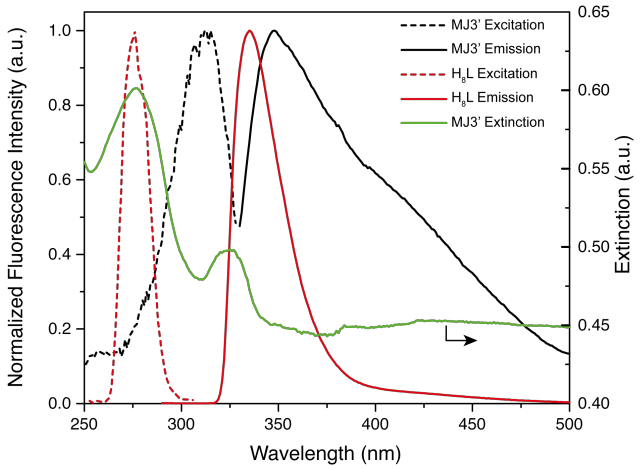

Figure 2. Normalized excitation and emission spectra of **MJ3'** in MeCN, and linker H_8L measured in DMF with the same excitation wavelength. The extinction of the MOF in solution is measured showing broadband scattering, and absorption peaks at c. 260 and 340 nm.

Method development and sensing of explosives with MJ3.

Explosives sensing was attempted with **MJ3'**. The sensing of explosives with MOFs in the solution-phase is useful, allowing the quantitative analysis of the MOF responses towards real explosive substances, as a proxy for vapor analysis. This in turn enables the measurement of sensor efficiency and mechanism, the sensitivity of the system, and performance comparisons to be made with other solution-phase MOF explosives sensors. In addition, a solution-phase sensing system has the potential to be used as an initial, rapid and cheap diagnostic tool for the in-field detection of explosive particles on a surface, or preconcentrated into a liquid sample, prior to their laboratory identification using analytical equipment such as liquid chromatography - mass spectrometry.

MOF **MJ3'** was tested against known quantities of explosive substances Tetryl, TNT, RDX, PETN and the TNT derivative and contaminant 2,4-DNT in MeCN solution. Suspensions of MOF **MJ3'** in MeCN were used for all solution-phase sensing experiments.

To test the physical stability of the **MJ3'** suspensions, a study was performed to investigate whether any of these particulates settled out of suspension during sensing. This is an important consideration as MOFs settling out of suspension cause an attenuation of the system's fluorescence creating ambiguity in the sensing data. The fluorescence emission of an **MJ3'** suspension left under constant illumination (315 nm) was measured every 60 seconds, for 4

minutes. Settling of the MOF does occur over this time-frame, resulting in the loss of fluorescence intensity (**Figure S3**).

To eradicate this problem, a vortexing procedure was implemented as described in the Methods. The MOF suspensions were subjected to 15 s of light agitation using a vortexer prior to each fluorescence emission reading. With the implementation of this vortexing procedure, consistent fluorescence emission intensities of **MJ3'** in suspension were obtained (**Figure S3**). Prior to any sensing experiment, settling and stable-baseline checks were implemented, if a sample did not achieve a stable base-line through vortexing, it would not be used in sensing. This effect, or measures to prevent such effects, have only occasionally been accounted for in MOF sensing literature.[25]

Another important factor to consider is the absolute amount of MOF material present within each tested suspension. Whilst the quenching responses calculated for each analyte are relative to the initial fluorescence intensity of a particular suspension sample, the amount of MOF material available to interact with the concentration of analyte added will affect the results obtained. Therefore, suspensions were always generated with the same amount of material and ultrasonicated for the same amount of time. It was observed that a 6 mg sample of finely ground **MJ3'** ultrasonicated for 2 hours gave the most stable suspensions and the initial fluorescence intensities (after the implemented settling and vortexing steps mentioned above) were consistent. In an attempt to mitigate for some of the discrepancies in absolute amount of MOF particulates in suspension, each sensing experiment for each analyte was repeated 3-5 times.

When sensing in the solution-phase using a particulate suspension, the final confounding factor that must be acknowledged is that of dilution. The 1 mM explosives stock solutions used for analyte sensing are produced through the further dilution of explosives standards using

MeCN, consequently, the effect of adding MeCN to the sensing suspension was evaluated to ensure that dilution was controlled for.

Figure 3 shows how the addition of 10 μL aliquots of MeCN does modify the fluorescence intensity of the MOF in suspension, causing some apparent quenching over and above dilution alone. Whilst this effect is small compared to the explosive quenching for the nitroaromatics, these effects do need to be considered when titrating the explosive substances against **MJ3'** and other MOFs. This effect is likely due to solvent addition destabilizing the particle suspension and might be remedied by smaller, more stable MOF particulates. Importantly, few literature sources explicitly claim to have accounted for the effects of dilution when expressing a suspended MOF sensors' response to an analyte, and in some instances it can be claimed that the observed responses are simply dilution effects.

Prior to the addition of the analyte to the MOF suspension, a steady initial fluorescence intensity baseline was obtained through implementation of three cycles of 15 s agitation of the MOF suspension using a vortexer. After this baseline was achieved, 10 μL of a 1mM solution of a particular analyte was added to the MOF in suspension in an incremental fashion until 100 μL of the explosive (or derivative) was added. After each 10 μL aliquot analyte addition, the vortexing step was repeated three times to ensure no settling of the MOF, generating three fluorescence emissions for each addition of an analyte. The three fluorescence intensities for each addition were averaged and a plot of the responses generated (**Figures S4 and S5**).

Figure 3 shows the baseline quenching percentage (QP) induced by MeCN and the QPs for each explosive as an average of at least 3 independent titration experiments, each completed on different suspension samples, all from different **MJ3'** synthetic batches and titrated against at least two independently made 1 mM explosives stock solutions. The order of the greatest

quenching of the MOF by the analytes follows Tetryl >> 2,4-DNT > PETN > TNT > RDX with uncorrected quench percentages at 62.5 μM of 59.7%, 37.2%, 36%, 32.6% and 26.2% respectively. Tetryl is observed to show significantly higher quenching responses in comparison to the other analytes.

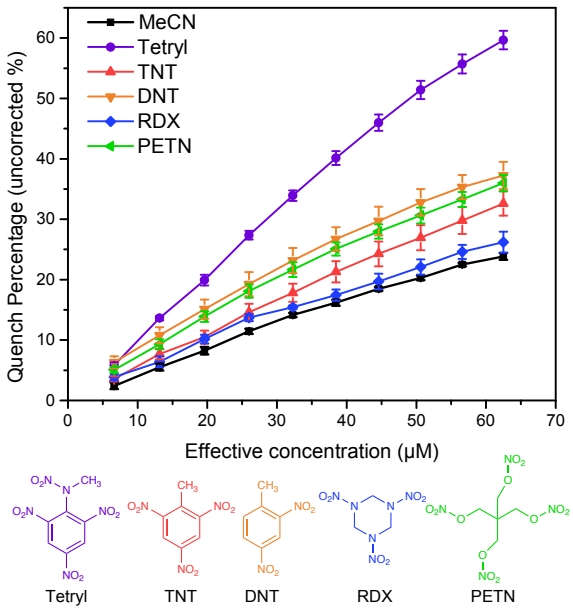

Figure 3. MJ3' suspensions in MeCN were quenched with addition of 1 mM solutions of various explosives. The full plots are shown in **Figure S4 and 5**. From these the percentage of quenching was calculated for each concentration, and additionally blank measurements were made on addition of pure MeCN to calculate a background, as shown. Error bars give 1 SE on the mean over at least 3 independent replicates. Explosive structures illustrated beneath.

Of particular note is the large quenching by PETN, which is one of the largest achieved to date by a MOF. We attribute this to the design of the large pore system allowing good access to the analyte. The quench percentages of 2,4-DNT and PETN are similar at multiple concentrations, meaning it would be difficult to differentiate which of these compounds were present in an unknown solution, and we return with a solution to this problem below. In addition

there is little or no difference between RDX and the dilution effects, suggesting the ability of RDX to quench **MJ3'** is limited, particularly at low concentrations tested here (**Figure S6**).

Quenching plots of I_0/I allow for an estimated rate of quenching to be determined and indicate simply whether multiple quenching processes are operating.[26] The plots for the five analytes are shown in **Figure S7**. The quenching plots for **MJ3'** upon exposure to TNT, 2,4-DNT, PETN and RDX are all linear, and this implies that only one type of quenching process is operative in these cases. Upon exposure to Tetryl however, **MJ3'** demonstrates a near liner plot at low concentrations (up to approximately 26 μM) followed by a clear deviation from linearity at higher concentrations. This suggests that two distinct quenching processes are likely to be causing the quenching of **MJ3'** upon exposure to Tetryl. As a result of the greater spectral overlap between the emission spectrum of the MOF and the absorption spectral of Tetryl, in comparison to the other tested analytes, it is suggested that some optical interactions could be responsible for the increased sensitivity towards this analyte with **MJ3'** (**Figure S8**). This has been previously observed for other MOFs, such as UiO-68@NH_2, with colored explosive solutions.[27]

The rates at which MOF **MJ3'** is quenched by the five substances can be seen in **Table S3**. These K_Q constants are circa $0.5 – 1.6\times10^4$ M^{-1}, of similar magnitude to those reported for the solution-phase sensing of explosives using state-of-the-art amplifying fluorescent conjugate polymers (AFCPs) as pioneered by Swager *et al.*[28] For example, one AFCP gave K_Q values of 4.3×10^3 M^{-1} and 1.1×10^4 M^{-1} upon exposure to TNT and 2,4,6-trinitrophenol in toluene solution respectively.[29] Another AFCP yielded K_Q values of 4.15×10^4 M^{-1} and 1.31×10^4 M^{-1} for TNP and 2,4-DNT respectively in tetrahydrofuran solution.[30] A comparison of the order of magnitude in

K_Q values suggests that **MJ3'** is as efficiently quenched by nitroaromatic compounds as AFCPs. The values are also in accordance with those reported for other MOF explosive sensors.[31]

The limits of detection (LOD) for each analyte upon the exposure of **MJ3'** are detailed in **Table S4**. All were in the micromolar range with, for example, DNT achieving an LOD of 3.2 μM (ca. 0.6 ppm).

Finally, to confirm that metal-organic framework **MJ3'** is not being degraded during sensing, a PXRD pattern of **MJ3'** in a sensing solution containing Tetryl (62.5 μM) was compared with a PXRD pattern of the MOF in MeCN solution. The same analysis was also completed on a 2,4-DNT + MOF sample (**Figure S9**). From these analyses no structural transformations of **MJ3'** were observed in the presence of these analytes.

Modelling of MJ3 interactions with explosives and related molecules.

As described above, in turn-off sensing the fluorescence of the MOF is quenched through the electron transfer from the conduction band of the MOF to the LUMO orbitals of the electron deficient analytes such as explosives. The lower the LUMO energy, the higher the electron affinity of the analytes and thus the higher the efficiency and magnitude of quenching of the MOF observed. Computational simulations of the electronic properties of **MJ3'** and the explosive substances (and related analytes) allow for naïve predictions to be made as to which analytes should quench the framework to the greatest extent through the photo-induced electron transfer mechanism (PIET).[11] The PBE0 functional used to calculate the MOF excitation energy differs very slightly from the measured optical band gap, possibly due to surface defects, temperature effects or flexibility of the MOF. The alignment of the ionization potentials (IPs) and electron affinities (EAs) of a range of analyte molecules and the MOF is displayed in **Figure 4a**. Whilst experimental data is limited to nitrobenzene, 2,4-DNT, 2,6-DNT and p-NT, the

calculated IPs of those analytes are within 0.2 eV of the literature values available,[32] while the EAs are consistently underestimated by 0.3 - 0.4 eV.[33,34]

From the results displayed, it is clear that the calculations predict that the quenching of fluorescence by electron transfer should occur in all analytes except DMNB, which possesses an EA above that of the MOF. However, if the above ~0.4 eV underestimation of EAs is included, this brings all the analytes below that of the MOF and so it could be expected that quenching in DMNB will occur as well. The order of quenching magnitude for the analytes tested here, based on these calculations should be Tetryl > TNT > 2,4-DNT > PETN > RDX. It should be noted that some deviation will be expected, due to the different electrostatic environments within the pore compared to vacuum, as well as any external factors influencing the MOF HOMO-LUMO positions unaccounted for in these calculations. The trends in **Figure 3** follow the order predicted in the modelling of energy levels, except for an under-quenching by TNT - it appears there is a lack of interaction between TNT and the MOF which is not accounted for in the theoretical calculations. This is unlikely to be a question of size due to the large pore diameters of the MOF, and the success of Tetryl and DNT with their similar structures. We speculate that there is a more complex interaction at play, perhaps a more subtle electronic misalignment or reaction between the MOF and analyte. Such differences between theoretical studies and the experimental results that arise when predicting MOF structure/function relationships, are of great interest for feeding back and improving models.[18] The modelling of MOF structure and electronics, as it becomes more accurate, will enable better prediction of suitable candidate MOFs for high throughput screening for sensing arrays.

In addition to the above, a further theoretical simulation of the charge density isosurface of the lowest unoccupied state calculated for the MOF with nitrobenzene in its pore (**Figure 4b**)

suggests an alignment of the analyte with the metal-organic framework. The electron density matches that of the LUMO of the nitrobenzene molecule, rather than the charge density of the conduction band of the empty MOF, indicating that electrons may transfer from the MOF to nitrobenzene. Full computational methods are given in the Supporting Information.

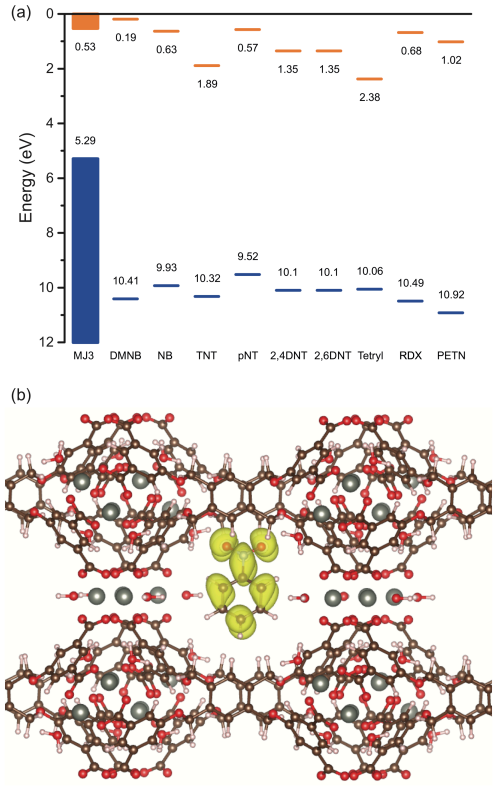

Figure 4. (a) Calculated alignment of the ionization energies and electron affinities of various molecules of interest with the HOMO/LUMO of MJ3. (b) Calculated charge density isosurface of the LUMO of MJ3 and pore bound-nitrobenzene.

Incorporation of MJ3 into a 3 MOF sensing array for explosives

To investigate whether to problem of explosive differentiation at variable concentration could be overcome, a sensing array of MOFs was created, featuring **MJ3'** alongside two literature MOFs, chosen to have contrasting sensing properties: Array MOF 2 (**AM2**) - [$Zn_2(oba)_2(bpy)$}•DMA]. H_2oba = 4,4'-oxybis(benzoate); bpy = 4,4'-bipyridine and DMA = N,N-

dimethylacetamide,[35] and Array MOF 3 (**AM3**) - [Eu(BTC)(H_2O)•1.5H_2O], where BTC = benzene-1,3,5-tricarboxylate.[36] The syntheses for **AM2** and **AM3** are illustrated in **Figures S10** and **S11**.

Metal-organic framework **AM2** was previously reported by Li *et al*.[35]. This three-dimensional MOF is constructed from $Zn_2(oba)_4$ paddle-wheel SBUs, and is noted to be porous with one-dimensional pores of approximately ~ 5.8 × 8.3 $Å^2$ running through the MOF. The calculated solvent accessible volume for the MOF was 25% and previous sensing experiments demonstrated **AM2** to be highly fluorescent and effective at detecting explosives-related nitroaromatic compounds (nitrobenzene, para-nitrotoluene, meta-dinitrobenzene, para-nitrobenzene and 2,4-DNT) in the vapour-phase. The MOF showed preferential quenching in the presence of smaller nitroaromatics such as nitrobenzene and demonstrated weak responses towards 2,4-DNT. In addition, the MOF demonstrated selectivity towards nitroaromatic compounds over interferents such as toluene, benzene and chlorobenzene; which were observed to increase the fluorescence of the MOF.[35] This MOF was chosen due to its reported lower sensitivity towards 2,4-DNT to yield a differential sensing response towards this analyte (as well as potentially the other larger explosives tested too) in comparison to **MJ3'**. Excitation was performed at 315 nm and emission was found to peak at 470 nm.

Metal-organic framework **AM3** is also previously reported.[36] In this MOF, europium atoms are bridged by the BTC linkers to form a 'three-dimensional rod packing structure'. The one-dimensional pores within this structure are reported to be of ~ 6.6 × 6.6 $Å^2$. This metal-organic framework demonstrates strong lanthanide luminescence (when excited at 285 nm) at 589, 615 and 700 nm which are attributed to the $^5D_0 \rightarrow {}^7F_1$, $^5D_0 \rightarrow {}^7F_2$ and $^5D_0 \rightarrow {}^7F_4$ transitions respectively. Chen *et al.* reported this MOF to be highly luminescent whilst suspended in MeCN,

and effective at detecting small molecules such as acetone. This was attributed by the group to the open metal sites present within the active MOF. This MOF was chosen as a component in the MOF sensor array owing to its stability in MeCN (the solvent used for the sensing procedures), as well as its strong lanthanide-based luminescence with open metal sites, that may provide an alternative quenching pathway from both the photo-induced electron transfer mechanism and the antennae screening effect, adding a potential differentiation pathway.[37] The relative structures of the array are given in **Figure S12** and the PXRDs confirming typicity are shown in **Figure S13**.

The 3 MOFs (**MJ3'**, **AM2** and **AM3**) were exposed to the same five explosives at a range of different concentrations and the luminescence quenching of each of the 3 MOFs caused by one explosive can be combined into a pattern or 'fingerprint' (**Figure S14**). If the explosive fingerprints remain unique at different concentrations of explosive, then it should be possible to discriminate between explosives at a range of different molarities. To analyze the multidimensional quenching patterns, the simple supervised learning technique Linear Discriminant Analysis (LDA) was used (**Figure 5**). LDA acts to maximize the between group (explosive in this case) separation whilst minimizing the within-group differences.[13,38] The models are then tested by LOOCV (leave one out cross validation) which removes each result in turn and tests the LDA model created with that result to see whether it is classified accurately or not.

With this 3 MOF array 100% classification was achieved using a fixed concentration of 62.5 μM. However, more usefully, as each MOF responds differently to the explosives at different concentrations, by grouping data by analyte and blinding the LDA model to concentration, good recognition can be achieved over ranges of concentrations down to 20 μM, with 82% classification achieved (**Figure 5d** - LOOCV). Even with as large a range as 62.5 – 6.6

μM reasonable classification was possible (75% by LOOCV, with increasing misclassification at the lower concentrations - **Figure S15**), showing that differentiation between analytes using the 3 MOFs is far more powerful than using one alone. The LDA technique works well at identifying single analytes or known mixtures with unique array outputs, however it should be noted that it is difficult to use for the determination of a continuous variable, hence he we have not attempted concentration determination here within groups.

Interestingly, it might be assumed that those analytes misclassified are likely to be the low concentration samples (as they tend towards pure solvent addition/dilution). However, on examination, it is seen that this is not always the case, and in many instances, particularly between DNT and TNT the occasional high concentration sample is confused, whereas low concentration data is well separated, suggesting future iterations of the array would benefit from an additional discrimination element working between DNT and TNT. It should also be noted that as the RDX signal is very low, there is a risk that on introduction of interferent materials that cause similar small changes in array PL, misclassification could occur. It is unlikely that due to the MOF design, anything other than a highly nitrated material would cause significant quenching of the array, but it should be possible to extend sensing to other explosives such as picric acid with this technology as well as formulations such as semtex (RDX/PETN) or pentolite (PETN/TNT).

Future work on this topic will focus on forming stable MOF suspensions in a multiplexed and high-throughput format, such combined MOFs in a well plate, resulting in an array that is highly cross-reactive, sensitive and selective, but also free from heavy metals such as Cd in previous quantum-dot based arrays.[7]

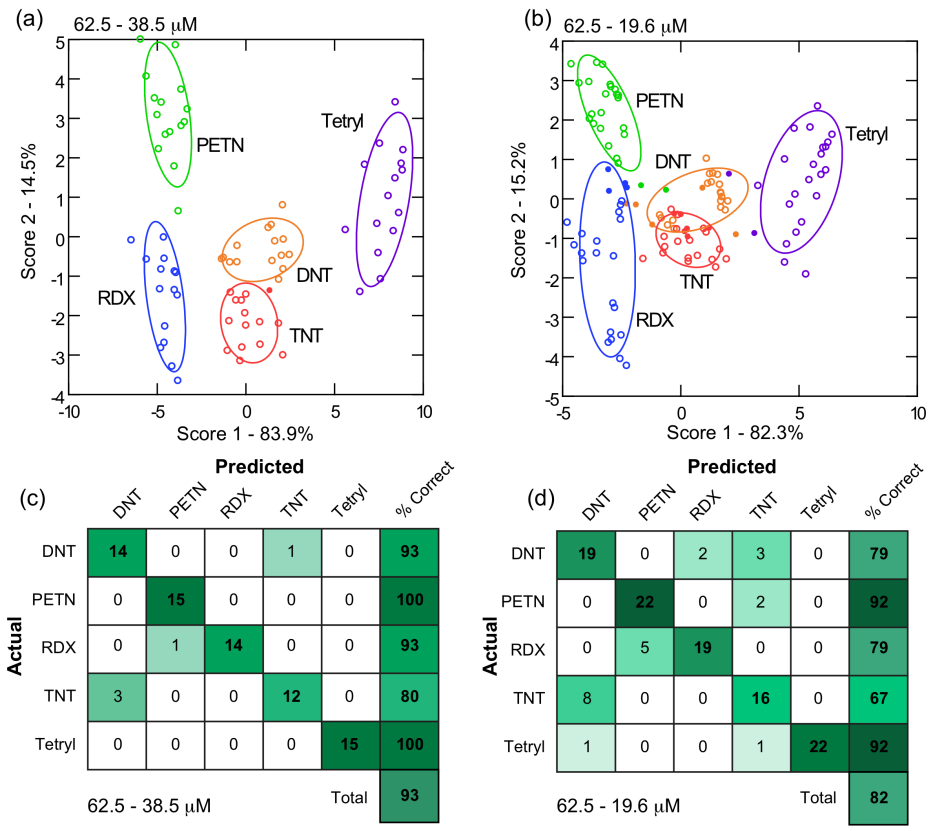

Figure 5. Canonical score plots and confusion matrices for the 3 MOF array over 2 different concentration ranges. (a, c) represent a smaller concentration range of 62.5 – 38.5 µM and (b,d) are for a larger range of 62.5 – 19.6 µM. The confusion matrices show the actual vs predicted values for each LDA model on the basis of LOOCV. Solid circles in the score plots indicate a misclassified data point. Ellipses are 1 SD on the cluster mean.

Conclusions

We have developed and demonstrated a new, large-pore MOF for explosives detection – **MJ3'**. We show good sensitivity and quenching constants for this material to a range of different explosives, and in particular have shown how a large pore size allows interactions with the difficult-to-detect PETN. Limits of detection were in the ppm range or below, suggesting utility for this material in environmental management and homeland security. We have also modelled the electronic states of the MOF and find a good match between theory and practice.

During the practical experiments, we have refined a methodology for solution phase sensing of explosives. We recommend this regime to the community to generate repeatable and accurate results, in particular to avoid artefacts caused by dilution and settling of MOF powders, as also advocated by other recent works.

Finally, we show for the first time, that by building a 3 MOF array it was possible to detect explosives whilst overcoming the limitations of analyte recognition confounded by concentration. Our array was able to reliably discriminate the five explosives over an order of magnitude of concentration. Future work will focus on the improvements of this system by multiplexing the array (we have selected emission wavelengths where this should be possible) and further fine tuning the MOF array with smaller, more stable particle suspensions, and by introducing more elements for improved sensitivity and discrimination.

Experimental Section

Materials and Instrumentation Materials and solvents were used as supplied from Sigma Aldrich and Alfa Aesar, with the exception of DMF, which was dried over molecular sieves (4Å). Explosive standards were provided at a concentration of 1 mg mL^{-1} by Accustandard in MeCN or MeCN/MeOH mixtures and diluted as appropriate. The standards were kept refrigerated in the dark at 4 °C and discarded within one month of opening.

Fluorescence excitation and emission measurements were made in 10 mm quartz cuvettes on a Horiba Fluoromax 4 instrument with a monochromated xenon arc light source. Instrument settings were kept consistent between all readings. Powder diffraction was performed on a STOE Stadi-P equipped with a Cu anode, Ge<111> monochromator (CuK_α λ=1.5418 Å) and a Dectris Mythen 1K detector. The data was collected in the transmission mode in the 2-45° 2θ range with

0.5° steps and data collection times of 20 s per step. Single crystal X-ray diffraction data were collected on a twin-source SuperNova diffractometer using a micro-focus Cu X-ray beam (50 kV, 0.8 mA) and an Atlas detector (135 mm CCD) (a detailed description of the crystallographic analyses can be found in the **Supplementary Information** document). NMR data were collected on a Brucker Avance 300 MHz instrument.

Synthesis of MJ3 and MJ3' MOF **MJ3** was synthesized from linker **H_8L** (synthesis described in the Supporting Information) in multiple batches. Zinc nitrate hexahydrate (0.1 mmol, 29.8 mg) was combined with **H_8L** (0.1 mmol, 85.5 mg) in 12 mL of DMF in a glass vial. The reaction mixture was stirred until the solution became clear, the vial was then crimp-sealed and placed in an oven set to 100 °C for 24 hours, affording clear, block-shaped crystals of **MJ3**. The DMF mother liquor was decanted off and MeCN was added, immersing the crystals in the solvent. The crystals were left to soak in MeCN for 24 hours, after which the solvent was pipetted off and MeOH was added, again to immerse the crystals. After a further 24 hours, the MeOH was replaced by acetone and the crystals were left for a further 24 hours. The final wash was conducted with CH_2Cl_2 for a final 24 hours. Post immersion in DCM, the solvent was decanted off and crystals were left to dry under dynamic vacuum, this yielded active **MJ3'**.

Solution phase testing overview A suspension of **MJ3'** was produced by weighing 6 mg of the dry crystals into 6 mL MeCN and sonicating in a bath sonicator for 3 hours. A 1 mL portion of this suspension was titrated with either 1 mM explosive solution or neat MeCN, in 10 μL increments to a total addition of 100 μL. Vortexing of the sample to prevent settling was undertaken between each repeat reading, and each addition step, as described in more detail in the Supporting Information.

Synthesis of AM2 and AM3 Array MOFs 2 and 3 were synthesized as per Pramanik *et al.*[35] and Chen *et al.*[36] respectively.

Statistical methods for array The three MOFs were individually exposed to each explosive at a range of concentrations in an identical manner described above for **MJ3'** following the same preparation and vortexing procedures during sample addition (also described further in the Supporting Information). Fluorescence data for each sequential addition of explosive, to give 10 concentrations, was collected for 3 independent repeats. This was performed for all three MOFs, where **MJ3'** was measured at 348 nm (ex 315 nm), **AM2** at 473 nm (ex 315 nm), and **AM3** at 589, 615 and 698 nm (ex 285 nm). The quench percentage was calculated for each measurement, at the appropriate wavelength ($1 - I/I_0$) and then corrected for the dilution of the MeCN based on standard curves collected independently. These corrected values were tabulated and used to build LDA models in Systat 13, using selected concentration ranges, grouped by explosive as the classifier. For example, to build the LDA model for Figure 5a, the input data matrix consisted of 5 explosives ×3 repeats ×5 concentrations ×5 MOF emissions; for Figure 5b, it is 5 explosives ×3 repeats ×8 concentrations ×5 MOF emissions.

ASSOCIATED CONTENT

Supporting Information

The Supporting Information is available free of charge on the ACS Publications website. Additional experimental information and methodology, computational methodology, supporting figures and crystallography tables (PDF)

Accession Codes

CCDC 1552177 contains the supplementary crystallographic data for **MJ3**. The data can be obtained free of charge via www.ccdc.cam.ac.uk, or by emailing data_request@ccdc.cam.ac.uk, or by contacting The Cambridge Crystallographic Data Centre, 12 Union Road, Cambridge CB2 1EZ, UK; fax: +44 1223 336033.

AUTHOR INFORMATION

Corresponding Author

* Email: william.peveler@glasgow.ac.uk

Author Contributions

∞ These authors contributed equally.

Notes

The authors declare no competing interests.

ACKNOWLEDGMENT

MJ acknowledges the EPSRC SECReT Doctoral Training Centre (EP/G037264/1). WJP was recipient of an EPSRC Doctoral Prize Fellowship (EP/M506448/1) and acknowledges the University of Glasgow for a Lord Kelvin Adam Smith Fellowship. DOS acknowledges funding through EPSRC (Grant No. EP/N01572X/1) and CNS is grateful to EPSRC and the Department of Chemistry at UCL for the provision of a Doctoral Training Partnership studentship (ref No. 1492829). The authors acknowledge the EPSRC for funding UCL's X-ray diffractometers (EP/K03930X/1). The DFT calculations in this article made use of the ARCHER U.K. National Supercomputing Service (http://www.archer.ac.uk), via our membership of the U.K.'s HEC

Materials Chemistry Consortium, which is funded by EPSRC (Grant No. EP/ L000202), and the UCL Legion (Legion@UCL) and Grace (Grace@UCL) HPC Facilities.

References

(1) Sun, X.; Wang, Y.; Lei, Y. Fluorescence Based Explosive Detection: From Mechanisms to Sensory Materials. *Chem. Soc. Rev.* **2015**, *44* (22), 8019–8061.

(2) Peveler, W. J.; Jaber, S. B.; Parkin, I. P. Nanoparticles in Explosives Detection - the State-of-the-Art and Future Directions. *Forensic Sci Med Pathol* **2017**, *13* (4), 490–494.

(3) ICX Technologies. *Fido Explosives Detectors Technical Overview*; PDF Online, 2011.

(4) Andrew, T. L.; Swager, T. M. A Fluorescence Turn-on Mechanism to Detect High Explosives RDX and PETN. *J. Am. Chem. Soc.* **2007**, *129* (23), 7254–7255.

(5) Madhu, S.; Bandela, A.; Ravikanth, M. BODIPY Based Fluorescent Chemodosimeter for Explosive Picric Acid in Aqueous Media and Rapid Detection in the Solid State. *RSC Adv.* **2014**, *4* (14), 7120–7123.

(6) Zwijnenburg, M. A.; Berardo, E.; Peveler, W. J.; Jelfs, K. E. Amine Molecular Cages as Supramolecular Fluorescent Explosive Sensors: a Computational Perspective. *J. Phys. Chem. B* **2016**, *120* (22), 5063–5072.

(7) Peveler, W. J.; Roldan, A.; Hollingsworth, N.; Porter, M. J.; Parkin, I. P. Multichannel Detection and Differentiation of Explosives with a Quantum Dot Array. *ACS Nano* **2016**, *10* (1), 1139–1146.

(8) Senthamizhan, A.; Celebioglu, A.; Uyar, T. Ultrafast on-Site Selective Visual Detection of TNT at Sub-Ppt Level Using Fluorescent Gold Cluster Incorporated Single Nanofiber. *Chem. Commun.* **2015**, *51* (26), 5590–5593.

(9) Jurcic, M.; Peveler, W. J.; Savory, C. N.; Scanlon, D. O.; Kenyon, A. J.; Parkin, I. P. The Vapour Phase Detection of Explosive Markers and Derivatives Using Two Fluorescent Metal–Organic Frameworks. *J. Mater. Chem. A* **2015**, *3* (12), 6351–6359.

(10) Banerjee, D.; Hu, Z.; Li, J. Luminescent Metal-Organic Frameworks as Explosive Sensors. *Dalton Trans.* **2014**, *43* (28), 10668–10685.

(11) Wang, S.; Wang, Q.; Feng, X.; Wang, B.; Yang, L. Explosives in the Cage: Metal-Organic Frameworks for High-Energy Materials Sensing and Desensitization. *Adv. Mater.* **2017**, *29* (36), 1701898.

(12) Woellner, M.; Hausdorf, S.; Klein, N.; Mueller, P.; Smith, M. W.; Kaskel, S. Adsorption and Detection of Hazardous Trace Gases by Metal–Organic Frameworks. *Adv. Mater.* **2018**, *30* (37), 1704679.

(13) Peveler, W. J.; Yazdani, M.; Rotello, V. M. Selectivity and Specificity: Pros and Cons in Sensing. *ACS Sens.* **2016**, *1* (11), 1282–1285.

(14) Ivy, M. A.; Gallagher, L. T.; Ellington, A. D.; Anslyn, E. V. Exploration of Plasticizer and Plastic Explosive Detection and Differentiation with Serum Albumin Cross-Reactive Arrays. *Chem. Sci.* **2012**, *3* (6), 1773–1779.

(15) Dunning, S. G.; Nuñez, A. J.; Moore, M. D.; Steiner, A.; Lynch, V. M.; Sessler, J. L.; Holliday, B. J.; Humphrey, S. M. A Sensor for Trace H_2O Detection in D_2O. *Chem* **2017**, *2* (4), 579–589.

(16) Hu, Z.; Pramanik, S.; Tan, K.; Zheng, C.; Liu, W.; Zhang, X.; Chabal, Y. J.; Li, J. Selective, Sensitive, and Reversible Detection of Vapor-Phase High Explosives via Two-Dimensional Mapping: a New Strategy for MOF-Based Sensors. *Cryst. Growth Des.* **2013**, *13* (10), 4204–4207.

(17) Campbell, M. G.; Liu, S. F.; Swager, T. M.; Dincă, M. Chemiresistive Sensor Arrays From Conductive 2D Metal-Organic Frameworks. *J. Am. Chem. Soc.* **2015**, *137* (43), 13780–13783.

(18) Gustafson, J. A.; Wilmer, C. E. Computational Design of Metal–Organic Framework Arrays for Gas Sensing: Influence of Array Size and Composition on Sensor Performance. *J. Phys. Chem. C* **2017**, *121* (11), 6033–6038.

(19) Küsgens, P.; Rose, M.; Senkovska, I.; Fröde, H.; Henschel, A.; Siegle, S.; Kaskel, S. Characterization of Metal-Organic Frameworks by Water Adsorption. *Microporous and Mesoporous Materials* **2009**, *120* (3), 325–330.

(20) Alaerts, L.; Séguin, E.; Poelman, H.; Thibault Starzyk, F.; Jacobs, P. A.; De Vos, D. E. Probing the Lewis Acidity and Catalytic Activity of the Metal–Organic Framework $[Cu_3(Btc)_2]$ (BTC=Benzene-1,3,5-Tricarboxylate). *Chem. Eur. J.* **2006**, *12* (28), 7353–7363.

(21) Al-Janabi, N.; Hill, P.; Torrente-Murciano, L.; Garforth, A.; Gorgojo, P.; Siperstein, F.; Fan, X. Mapping the Cu-BTC Metal–Organic Framework (HKUST-1) Stability Envelope in the Presence of Water Vapour for CO2 Adsorption From Flue Gases. *Chemical Engineering Journal* **2015**, *281*, 669–677.

(22) Li, M.; Li, D.; O'Keeffe, M.; Yaghi, O. M. Topological Analysis of Metal–Organic Frameworks with Polytopic Linkers and/or Multiple Building Units and the Minimal Transitivity Principle. *Chem. Rev.* **2013**, *114* (2), 1343–1370.

(23) Eubank, J. F.; Mouttaki, H.; Cairns, A. J.; Belmabkhout, Y.; Wojtas, L.; Luebke, R.; Alkordi, M.; Eddaoudi, M. The Quest for Modular Nanocages: Tbo-MOF as an Archetype for Mutual Substitution, Functionalization, and Expansion of Quadrangular Pillar Building Blocks. *J. Am. Chem. Soc.* **2011**, *133* (36), 14204–14207.

(24) Gole, B.; Bar, A. K.; Mukherjee, P. S. Fluorescent Metal-Organic Framework for Selective Sensing of Nitroaromatic Explosives. *Chem. Commun.* **2011**, *47* (44), 12137–12139.

(25) Palomba, J. M.; Credille, C. V.; Kalaj, M.; DeCoste, J. B.; Peterson, G. W.; Tovar, T. M.; Cohen, S. M. High-Throughput Screening of Solid-State Catalysts for Nerve Agent Degradation. *Chem. Commun.* **2018**, *54* (45), 5768–5771.

(26) Chen, J.-K.; Yang, S.-M.; Li, B.-H.; Lin, C.-H.; Lee, S. Fluorescence Quenching Investigation of Methyl Red Adsorption on Aluminum-Based Metal–Organic Frameworks. *Langmuir* **2018**, *34* (4), 1441–1446.

(27) Nagarkar, S. S.; Desai, A. V.; Samanta, P.; Ghosh, S. K. Aqueous Phase Selective Detection of 2,4,6-Trinitrophenol Using a Fluorescent Metal-Organic Framework with a Pendant Recognition Site. *Dalton Trans.* **2015**, *44* (34), 15175–15180.

(28) Thomas, S. W. I.; Joly, G. D.; Swager, T. M. Chemical Sensors Based on Amplifying Fluorescent Conjugated Polymers. *Chem. Rev.* **2007**, *107* (4), 1339–1386.

(29) Sohn, H.; Sailor, M. J.; Magde, D.; Trogler, W. C. Detection of Nitroaromatic Explosives Based on Photoluminescent Polymers Containing Metalloles. *J. Am. Chem. Soc.* **2003**, *125* (13), 3821–3830.

(30) Saxena, A.; Fujiki, M.; Rai, R.; Kwak, G. Fluoroalkylated Polysilane Film as a Chemosensor for Explosive Nitroaromatic Compounds. *Chem. Mater.* **2005**, *17* (8), 2181–2185.

(31) Hu, Z.; Deibert, B. J.; Li, J. Luminescent Metal–Organic Frameworks for Chemical Sensing and Explosive Detection. *Chem. Soc. Rev.* **2014**, *43* (16), 5815–5840.

(32) Qasim, M.; Kholod, Y.; Gorb, L.; Magers, D.; Honea, P.; Leszczynski, J. Application of Quantum-Chemical Approximations to Environmental Problems: Prediction of Physical and Chemical Properties of TNT and Related Species. *Chemosphere* **2007**, *69* (7), 1144–1150.

(33) Chowdhury, S.; Heinis, T.; Grimsrud, E. P.; Kebarle, P. Entropy Changes and Electron Affinities From Gas-Phase Electron-Transfer Equilibria: $A^- + B = a + B$. *The Journal of Physical Chemistry* **1986**, *90* (12), 2747–2752.

(34) Desfrançois, C.; Périquet, V.; Lyapustina, S. A.; Lippa, T. P.; Robinson, D. W.; Bowen, K. H.; Nonaka, H.; Compton, R. N. Electron Binding to Valence and Multipole States of Molecules: Nitrobenzene, Para- and Meta-Dinitrobenzenes. *J. Chem. Phys.* **1999**, *111* (10), 4569–4576.

(35) Pramanik, S.; Zheng, C.; Zhang, X.; Emge, T. J.; Li, J. New Microporous Metal−Organic Framework Demonstrating Unique Selectivity for Detection of High Explosives and Aromatic Compounds. *J. Am. Chem. Soc.* **2011**, *133* (12), 4153–4155.

(36) Chen, B.; Yang, Y.; Zapata, F.; Lin, G.; Qian, G.; Lobkovsky, E. B. Luminescent Open Metal Sites Within a Metal–Organic Framework for Sensing Small Molecules. *Adv. Mater.* **2007**, *19* (13), 1693–1696.

(37) Zhou, X.; Li, H.; Xiao, H.; Li, L.; Zhao, Q.; Yang, T.; Zuo, J.; Huang, W. A Microporous Luminescent Europium Metal-Organic Framework for Nitro Explosive Sensing. *Dalton Trans.* **2013**, *42* (16), 5718–5723.

(38) Stewart, S.; Ivy, M. A.; Anslyn, E. V. The Use of Principal Component Analysis and Discriminant Analysis in Differential Sensing Routines. *Chem. Soc. Rev.* **2014**, *43* (1), 70–84.

TOC Graphic:

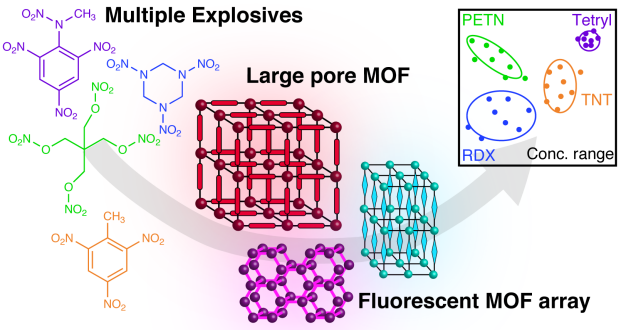
Multiple Explosives
Large pore MOF
Fluorescent MOF array
PETN
Tetryl
TNT
RDX
Conc. range